NASA Contractor Report 195056

ICASE Report No. 95-16

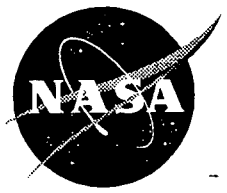

ICASE

IMPLEMENTATION OF A PARALLEL UNSTRUCTURED EULER SOLVER ON THE CM-5

E. Morano
D. J. Mavriplis

Contract No. NAS1-19480
March 1995

Institute for Computer Applications in Science and Engineering
NASA Langley Research Center
Hampton, VA 23681-0001

Operated by Universities Space Research Association

IMPLEMENTATION OF A PARALLEL UNSTRUCTURED EULER SOLVER ON THE CM-5*

E. Morano and D. J. Mavriplis
Institute for Computer Applications in Science and Engineering
MS 132C, NASA Langley Research Center
Hampton, VA 23681-0001 USA

ABSTRACT

An efficient unstructured 3D Euler solver is parallelized on a Thinking Machine Corporation Connection Machine 5, distributed memory computer with vectorizing capability. In this paper, the SIMD strategy is employed through the use of the CM Fortran language and the CMSSL scientific library. The performance of the CMSSL mesh partitioner is evaluated and the overall efficiency of the parallel flow solver is discussed .

*This research was supported by the National Aeronautics and Space Administration under NASA Contract No. NAS1-19480 while the authors were in residence at the Institute for Computer Applications in Science and Engineering (ICASE), NASA Langley Research Center, Hampton, VA 23681-0001. The first author was also partially supported by INRIA, "Région Provence-Alpes-Côte d'Azur" (France).

1 INTRODUCTION

Computer technology has grown rapidly over the last several years especially with regard to parallel architectures. Such machines are becoming useful for solving very large computational fluid dynamics problems, such as inviscid and viscous three dimensional flows about complex configurations, using upwards of one million grid points.

Since many different architectures have been developed and are available, efficient solution techniques and software are required which are adapted to the computational problem and also to the particular machine. There are essentially two requirements: the software must be parallelizable and here, also vectorizable, since each processing node of the CM-5 partition contains 4 vector units (VU's). For example, a Jacobi cycle is suitable, but a Gauss-Seidel iteration is not inherently vectorizable. This vectorization is provided by the compiler and does not require any explicit colored-type implementation. Moreover, the algorithm must also be efficient enough [1, 2], that is, must require a minimum number of operations to obtain a converged solution. In the case of unstructured meshes, only a few algorithms satisfy these requirements. In this work, it will be shown how a multistage explicit 3D Euler solver may be implemented on the CM-5 machine.

The CM-5 architecture can be used as a Single Instruction Multiple Data (SIMD) machine or as a Multiple Instruction Multiple Data (MIMD) machine. In the first approach each processing node performs the same instructions but on different data elements, while in the second approach, each processing node executes different instructions on different data sets. The SIMD approach on the CM-5 will be studied in this paper. This is done by making use of the CM Fortran (CMF) language. This language is an extension of the Fortran 90 language and has the particularity of treating entire arrays as variables. It provides a much more compact way of programming. Moreover, on the CM-5 computer, the programmer may access a large set of libraries: CM Fortran Utility Library [3] and Connection Machine Scientific Software Library (CMSSL [4]) for CM Fortran [5]. The first library provides subroutines such as "CMF_fe_array_from/to_CM" to use, or to produce, CM-objects instead of writing lower-level software. The second library is related to the use of scientific functions such as the manipulation of CM-arrays: L2 vector/matrix norms and the gather/scatter operations for sparse matrices, for example, which are required here.

While this programming model gives the illusion of an SIMD architecture, the global CMF code is in fact transformed by the compiler into an MIMD program which is then run simultaneously on each processor.

Since the memory is distributed on this machine, each VU has its own memory where the data elements are located and the distribution of the data elements over the vector units can strongly affect the overall performance, because of the time required for the interprocessor communication. Therefore, a partitioner provided in the CMSSL library, developed by Johan [4, 6], will be used with a slight modification.

All codes are compiled using CMF 2.1.1.2 and CMSSL 3.2. They are run on a CM-5 computer with 128 processing nodes (512 VU's) under CMOST 7.3 Final 1 Rev 3. All the examples run on the latter system are timeshared for the 32 and 64 processing node executions, while they are run in dedicated mode for the 128 processing node executions: this allows the use of the entire available memory (3.48 GBytes) for a single job. Each 32 node partition represents 891 MBytes of memory, the difference between the original 1 GByte and the 891 MBytes is due to the overhead. All reported timings correspond to CM-Busy times. This work was introduced in [7] with slight differences.

2 UNSTRUCTURED SOLVER

The basis for the implementation is a three dimensional unstructured single-grid Euler solver. Unstructured meshes provide the most flexible means for the discretization of complex domains and for adaptation of the mesh to flow features. Since an explicit scheme may be considered as the product of a sparse matrix by a vector, unstructured meshes result in (very) large sparse matrices and therefore require the use of gather/scatter operations to enable vectorization and/or parallelization.

Venkatakrishnan et al. in [8] implement a mesh-vertex finite volume upwind scheme for solving the Euler equations on triangular unstructured meshes on the Intel iPSC/860, an MIMD computer. A four-stage Runge-Kutta scheme is used to advance the solution in time. Farhat et al. in [9] propose the discretization of the 2D Navier-Stokes equations using a second order accurate monotonic upwind scheme for conservation laws (MUSCL) on fully unstructured grids. The spatial approximation combines an upwind finite volume method for the discretization of the convective fluxes with a Galerkin finite element method for the discretization of the diffusive fluxes. The time integration is performed through an explicit second order Runge-Kutta scheme and the code is implemented on a CM-2 computer. Johan et al. in [10, 6] solve the 3D Euler equations with a finite element program implemented on the CM-5 in CM Fortran. The variational form is based on the Galerkin/least-squares formulation. They use an implicit scheme to converge the solution to steady state. A matrix-free GMRES technique is used to solve the linear system at each time-step. More recently, Farhat et al. in [11] proposed the evaluation of different massively parallel architectures through the simulation of unsteady and steady viscous flows on the iPSC-860, the CM-5 and the KSR-1 computers. The discretization relies on a mixed finite element/finite volume formulation on unstructured meshes. The spatial approximation combines a Galerkin approximation for the viscous terms and an upwind Roe scheme for the convective fluxes. Second order solutions are provided through a MUSCL (Monotonic Upwind Scheme for Conservative Laws) approach. The time integration is achieved through a 3 stage variant of the Runge-Kutta method. Message Passing codes are implemented on the machines and an SIMD version of the solver is also implemented on the CM-5. The performances confirm the results presented in [7]: 107 MFlops on a 392161 edge based unstructured 2D mesh using 32 processing nodes.

This work was already partially introduced in [7] and the sequential version of this algorithm has been already reported in [12]. A parallel version was implemented on the Intel iPSC/860 hypercube using the PARTI primitives [13]. The equations are discretized on the unstructured mesh using a Galerkin finite-element formulation. The flow variables are stored at the vertices of the mesh, and piecewise linear flux functions are assumed over the individual tetrahedra of the mesh. The scheme is a so-called central differencing scheme [14]. Artificial dissipation, constructed as a blend of a Laplacian and biharmonic operator, is added to maintain stability. The main data-structure of this code is an edge-based data-structure. Residuals are constructed by executing loops over the edges of the mesh. At mesh boundaries, an additional loop over the triangular faces which form the boundary is then performed. The resulting spatially discretized equations must be integrated in time to obtain the steady-state solution. This is achieved using a 5-stage Runge-Kutta scheme. More details of this scheme are available in [12].

3 PARTITIONING OF DATA

As mentioned in the introduction, the memory is distributed over all the VU's (each processing node has 4 VU's). Thus, it is necessary to understand how, in the processors, the memory is managed and how the vectorization is performed, and both must be worked out together. These will be illustrated through the following example.

An array containing 2800 data elements is to be distributed on a CM-5 comprising 32 processing nodes, that is 128 vector units, each of them managing its own memory. The quotient of the division of 2800 by 128, i.e. 21, should be the number of data per VU. Actually, in order to distribute the data, two features are available.

- There is what can be called "the rule of 8". The length of the pipeline of a vector unit is equal to 8, thus the size of the data to be distributed on each VU has to be a multiple of 8. 21 is obviously not a multiple of 8 and the next number multiple of 8 is 24. The quotient of the division of 2800 by 24, i.e. 116, represent the number of VU's that will contain 24 data, the remaining data (2800-(116*24) = 16) goes in the 117-th VU. As explained in [4], the first 24 data will be allocated to the first VU, the second 24 data to the second VU and so forth... In this example only 117 VU's are used, instead of

128, and the array is not large enough to fit the machine correctly. However, this problem disappears for larger meshes.

- Another feature of the last released CMSSL library is that this rule of 8 is no longer mandatory to ensure proper vectorization. The only requirement is that the length of each data set in each VU be a multiple of a positive power of 2. The previous example is considered as follows: 21 is not a multiple of any positive power of 2, while 22 is. Hence, the number of VU's containing 22 data is 127, the remaining 6 data being assigned to the 128th VU. In this case, all the VU's are being used which results in an excess of communication time with respect to the computational time. Here again, this problem tends to disappear when the size of the mesh increases for a given architecture. In order to use this option, the partitioner and the solver software must be compiled with the "-nopadding" option (for further details see in [15]).

The partitioner provided in the CMSSL library is designed to partition Finite Element meshes: for clarity a 2D mesh, built with triangles, is considered. In order to use the partitioner, the graph to be partitioned needs to be described. In the CMSSL library, since the triangles are partitioned, the graph considered is the dual to the triangulation where each triangle is represented as a vertex in the graph. The graph is defined by the array "idual":

idual(m,n) =
- the number of the triangle that shares the face m with the triangle n.
- 0 if there is no neighbour (i.e. at the boundary).

In the present case, the vertices of the triangulation are partitioned rather than the triangles. Therefore, the graph to be partitioned is the triangulation itself. The graph is thus described in terms of nodes connected by edges. First to be determined is the maximum number of neighbors a node may have (max_ngh) all over the mesh, then the actual number of neighbors for each node (act_ngh). The graph is built using the array "idual" defined as:

idual(m,n) =
- the number of the edge that shares the node m with the edge n.
- 0 if n > act_ngh.

The partitioning is achieved through the use of a parallel recursive spectral bisection (RSB) implemented in CMF by Johan et al. [6]. The call of the routine "Partition_Mesh" will provide a new numbering of the nodes of the mesh through an array of permutation. It is important to note that the RSB partitioner implemented in the CMSSL library does not necessarily ensure a unique solution. Therefore, two runs on the same graph usually produce two slightly different results [6].

Since most of the computation is based upon edge loops, edges are the primary representation of the mesh and, once the permutation array is obtained, the edges are partitioned. An edge is represented by its origin and extremity. If both nodes of an edge belong to the same processor, then the edge is allocated to that same processor. If the two end nodes of an edge reside in different processors, the edge is then allocated to one of the two processors. Since either processor can be chosen, at this point, the edges are assigned in a manner which ensures even size partitions of edges for each processor. For example, in Fig.1, is shown the case of a 2D mesh, and how, from the original mesh and through the edges, the renumbering is achieved. The mesh comprises 25 nodes and 56 edges. The "Partition_Mesh" routine provides then 3 partitions with 8 nodes each and 1 partition with 1 node. The boundary between each partition is depicted by the thick dash line.

In an unstructured mesh, the way the edges are to be distributed depends strongly on the connectivity of each node (number of connecting neighbors). Therefore, one processor may receive a greater number of edges than another. This results in non-equal length sets of data. In order to ensure proper data distribution and to provide maximum computational rates, dummy data elements called "zeros", since they are actually zero

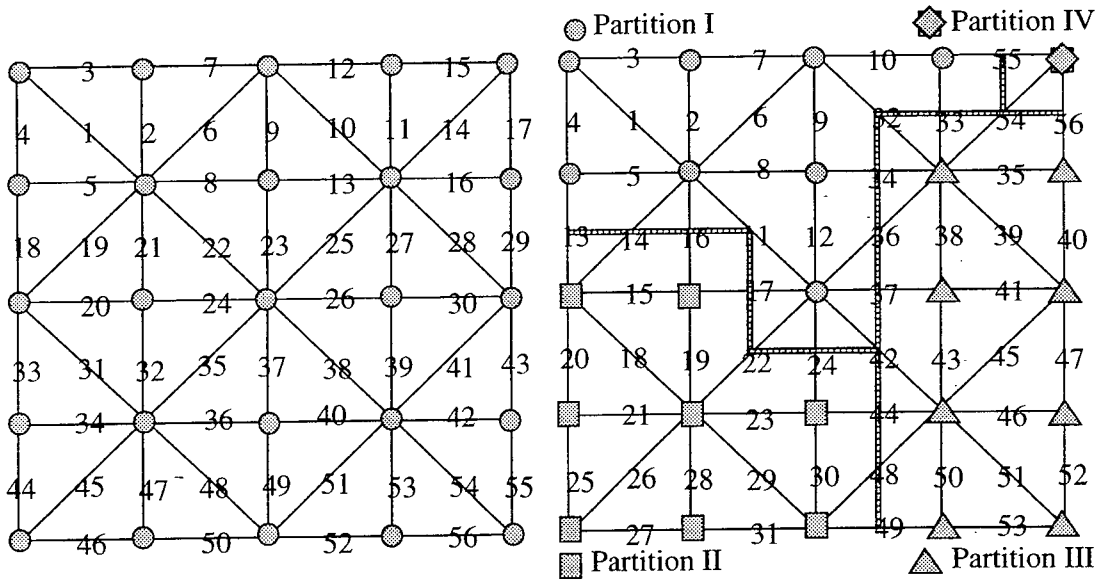

Figure 1: Partitioning Example.

valued data elements during the computation, are added to each partition. When the VU pipeline length is 8, it is important to employ partitions in which the data sets are multiples of 8, in order to maximize the VU computational rates. In general, the partitions will not naturally be divisible by 8. Therefore, the "zeros" are added such that the number of edges per processor be divisible by 8.

A similar partitioning is carried out for the triangular boundary faces, since these form the basis of the boundary condition loops. Since the number of boundary faces is smaller than the number of mesh edges (see Table 2.B for example) they do not affect the computation significantly. Yet, it is useful to note that each face (actually a face is represented by a tetrahedron, since the interior node needs to be known for computational purposes) is comprised of 4 nodes. Each of these nodes may be on a different processor, hence the number of "zeros" to be added per node is proportionally greater than for the edges. This number may be regarded as much smaller than the number of edges but is not negligible.

The number of nodes is obviously not affected by the previous methods and remains the same as before the partitioning.

The following particular ratio is to be of some importance:

$$edge\_ratio = \frac{cut\_edges\_part}{max\_edges},$$

where *cut_edges_part* is the number of cut edges, divided by the number of partitions, and *max_edges* the maximum number of edges strictly included in a processor. The quantity *cut_edges_part* represents a good metric of the interprocessor communication time and *max_edges* a good metric of the pure computational time. This ratio will govern the overall performance of the code. A similar *face_ratio* may have been studied but was not considered for clarity purpose. The only cases where such a ratio could be considered significant is when the faces represent more than 20 % of the computational operations. This happens when small meshes are distributed on a large number of processors which obviously becomes rapidly inefficient and therefore need be neither used nor studied.

Several results obtained with the partitioner applied to an ONERA M6 wing mesh (Fig.8) and a mesh over an aircraft configuration (Fig.10) are discussed. The meshes being used are described in Table 1.

Tables 2 to 4, showing partitioner execution summary, are to be read as follows:

- The size of the meshes is expressed as the number of nodes, edges (the most relevant data) and boundary faces before being partitioned.
- The memory required to run the code is obtained by including "isys = system('cmps')" as the last command line in the code. The result of the sum of the VU heap and stack is expressed in KBytes per VU. In order to obtain the memory allocated to run the code on the entire machine it is necessary to multiply the value by the number of VU's (a division by 1024 gives the value in MBytes).
- CPU times are measured for the execution of the "Partition_Mesh" CMSSL subroutine and for the total partitioning process, that is for "Partition_Mesh" and for renumbering and reordering the edges and the faces (I/O operations are not considered).
- The *edge_ratio*: for a given geometry, it is expected that the statement "the bigger the mesh the better" will hold. Indeed, the density of nodes increases faster than the interprocessor boundary size; hence, the value of *edge_ratio* decreases for larger meshes. Therefore more CPU time will be spent in the computation compared to the communication, and the global performance will improve.
- The resulting number of edges and faces after the partitioning process (due to the addition of the "zeros").
- The percentage of the number of faces over the number of edges.

One particular feature of the CM Fortran available on the CM-5 is that it supports a dynamic array allocation. This feature has been used in the last release of the code used here to partition the data. The interest of the use of the dynamic array allocation resides in a more flexible way to run the code. It becomes unnecessary to re-compile it prior to each run. The main difficulty concerns the precise measurement of the memory through the use of the "cmps" command. Indeed, this command gives the status of the system when requested, hence the possible lack of precision due to the fact that some arrays might not be allocated at this time.

Tables 2.A to 2.E show the partitioner execution summary for the 32 node configuration computer respectively for:

1. The rule of 8.
2. The rule of 8 with the "low-storage" option, an option that allows a smaller memory allocation requirement than the "default-storage" option, (the latter of which was used exclusively in [7]. However, the "low-storage" option requires more CPU time (see [15]).
3. The "-nopadding" option.
4. The "-nopadding" and "low-storage" options.

Tables 3 and 4 depict the results for the 64 and 128 node configuration respectively.

As for memory measurements, the results in Table 2.A and the results reported in [7] appear slightly different but nevertheless consistent. This difference may result from the present use of the dynamic array allocation (in [7] this feature was not used), but also from the new operating system, the new CMSSL library and maybe from the non-uniqueness of the solution of the "Partition_Mesh" subroutine (i.e. the resulting mesh is possibly larger or smaller than those shown in [7]). The increase of the number of edges ranges from 0.7 % to 21 %. The larger the mesh on a given configuration the lower the increase because the density of

inner processor edges is larger. For a given mesh the larger the number of processing nodes the larger the increase since the same number of edges has to distributed on a larger number of processors. The increase of the number of faces follows the same rules but at a much higher degree (from 98% to as high as 287 % !), since a face can be shared by as many as 4 different VU's (this case does not generally appear and 3 seems to be the maximum). The "Partition_Mesh" subroutine requires 20–50 % of the total partitioning process. This is explained by the fact that the code is not entirely parallelized. Complete parallelization would require a large amount of communication and dramatic reductions in CPU time cannot be expected. When the "low storage" option is used, the "Partition_Mesh" subroutine requires 50 % more time, but the memory requirements are only 65 % as of those required as with the "default storage" option.

In Fig.2, the memory requirements with respect to the number of edges for each available option on the 32 node machine are depicted. A simple extrapolation (curves are linear) shows what the 2403874 edge mesh would require in terms of memory and time. The memory requirement can be attained with the 64 node machine using the "low storage" option with either the "-nopadding" or the "rule of 8" options, which requires 1.39 or 1.44 GBytes respectively. Although the CPU time does not appear to be a limitation a priori, it is obviously preferable, when possible, to use the "default storage" option. The time required to partition the 2403874 edge mesh cannot be extrapolated as easily since partitioning the same mesh on a larger architecture increases communication but provides better computational performance, and the balance between these two factors is not a priori known. As shown in [6], time is not a linear function of the number of processing nodes. Therefore, the options are in favor (slightly !) of the "low storage" and the "-nopadding" for the memory requirement.

The results for the 64 node runs are presented in Table 3. The memory requirement for the 2403874 edge mesh, with 1.32 GBytes, proves the previous estimation to be valid. The same type of results are shown on Table 4 for the 128 node partition, where no limitation was found for the presented meshes.

It is clear, and expected, that the "edge_ratio", for a given geometry, decreases when the mesh gets larger. Yet, this "edge_ratio" increases when the configuration of the machine gets larger. Indeed, a given mesh is partitioned on a greater number of processors thus creating more interprocessor boundaries. Therefore, it is expected that the overall computational performance will be "optimal" when this "edge_ratio" will be minimum. As for the aircraft configuration, despite a greater number of edges (697992) versus the second largest M6 wing (353476), a great improvement in terms of performance cannot be expected since their respective values of the "edge_ratio" are similar.

4 PERFORMANCE RESULTS

In the Tables 5 to 8 results are presented as follows:

- Meshes are represented by their number of nodes, edges and faces.
- The memory requirement is expressed in KBytes per VU. This is obtained through the command line "isys = system('cmps')" as for the partitioner. Since this code does not use dynamic array allocation memory, the memory measurements should be more accurate than those of the partitioner.
- The CPU time entry contains two columns: the first one represents only the computational time whereas the second takes into account the computational time and the communication time which is included in the gather/scatter operations. These operations are performed through the use of the following routines available in the CMSSL library [4]:
  - "Part_Gather/Scatter" for single dimension arrays,
  - "Part_Vector_Gather/Scatter" for multiple dimension arrays.

  The CPU time is expressed as an average computed over 100 iterations.

- The overall performance of the code is expressed in MFlops.

As for memory requirements, here again, the results in Table 6.A are consistent with those that appear in [7]. The previous remarks concerning the differences related to the partitioner still apply.

As seen in Table 5, computations done directly without partitioning the meshes reflect that partitioning does improve the overall performance of the code. For example, although the non-partitioned 353476 edge mesh is smaller than the partitioned 360448 edge mesh (addition of "zero-edges" and "zero-faces" in the partitioned mesh) the memory allocation needed by the gather/scatter routines is larger. Indeed, since the nodes are randomly distributed among the processors, the number of cut edges is larger and the gather process produces more duplications. The computational times are of the same magnitude for both meshes. On the other hand, the total time shows a 7-fold increase resulting in low overall performance.

Even in the partitioned cases, shown in Tables 6 to 8, the computational time is around 10 times smaller than the total time. Therefore, pure computational performance of about 1 GFlops are dramatically reduced to 104 MFlops. The communication time in all these cases is much larger than the computation time. Thus, the overall computational rates of 20 MFlops per processor achieved by Johan [6] cannot be expected nor achieved. Yet, an average of 0.8 Mflops per processor attained here are similar to those presented in [11]. Indeed, the codes used in [7] and [11] are somehow similar with respect to the discretization and the time marching algorithm.

Table 9 depicts the execution summary of the code during one iteration, routine by routine where the computational performance is pointed out: STEP represents the computation of the time step, DEFLUX (D) the artificial diffusion, DEFLUX (C) the convection fluxes, PSMOO the residual smoothing and MONITR the computation of the RMS average of all flow field residuals. The values are given in the first Runge-Kutta step for DEFLUX (D), DEFLUX (C) and PSMOO. In the PSMOO subroutine, two iterations of a Jacobi iterative process (implicit residual averaging, see [16]) are performed over the whole mesh and the result is the average. STEP and MONITR are calculated respectively at the beginning and at the end of the global iteration. The mesh used is the partitioned 360448 edge mesh of the M6 wing. The various computations are performed over edges, faces and nodes. This table shows the CPU times required for the gather operation, the computation and the total time including gather, computation and scatter. The gather bandwidth for double precision data is calculated by dividing the number of bytes transferred (either within a processor or between processors) by the time used to do so. For example, the number of transferred data from an array A(5,mnode) to an array GA(2,5,medge), where 5 is the number of variables in 3D, mnode the number of nodes and medge the number of edges, amounts to a total of 2 x 5 x medge x 8 bytes. The gather bandwidth per processing node for the edges results in 15 Mbytes/s for each routine. When the performances obtained with the computational time only (MFlops (C)) are compared to the total time (MFlops (T)), it is easily seen that performance considerably deteriorates in the particular subroutines which include large portions of communication. The pure computational performance is pointed out since more than 1 GFlops for computation only are obtained. Therefore, these results show that the compiler provides a good vectorization of the code and that the communication rates are similar to those achieved by Johan in [6] which ensures that the meshes are well partitioned. The deterioration is due to the large number of communication steps used in each routine.

Fig.3 shows the memory requirement of the solver, expressed in MBytes, with respect to the number of edges of each mesh, for the three possible configurations of the machine (32, 64 and 128 processing nodes). For the 32 node configuration, since the 2403874 edge mesh could not be neither partitioned nor run with the solver, an extrapolation has been performed. The theoretical size of the partitioned mesh is extrapolated from the results obtained in Table 2.E and results in a 2432489 edge mesh. Then, its memory requirement is extrapolated from results obtained in Table 6.C. It shows clearly that such a computation is possible neither with the 32 node machine nor with the 64 node configuration. Indeed, the double and triple dash lines show respectively the available memory for the 32 and the 64 node configuration. It is also interesting to note that the 3 curves are almost the same, demonstrating again the quality of the partitioning process. The previous

remarks are also reflected in Fig.4, where the memory requirements, expressed in MBytes, are presented with respect to the number of processors for each initial mesh. Again, the memory requirement expressed for the 357900 node mesh on the 32 and 64 node machine are only extrapolations, and as expected the computation of the 2433280 edge mesh (see Table.3) could not be achieved on the 64 node machine.

Fig.5 depicts the overall performance with respect to the number of edges for the three possible configurations of the machine (32, 64 and 128 processing nodes). As for the 32 and 64 node configuration, the overall performance shows a rapid stall when the number of edges increases, confirming the increase of communication time. In these cases, the results obtained with the largest number of edges correspond to the aircraft configuration mesh, while the results of the second largest number of edges correspond to the second largest M6 wing mesh, thus they may not reflect the real attainable performance. However, and as a confirmation of the previous assumption, when these measures are performed with the 128 node machine, the stall appears as well with the largest mesh which discretizes the same M6 wing.

The overall performance with respect to the value of the *edge_ratio* is depicted in Fig.6. The number of MFlops is seen to be strongly related to the value of the *edge_ratio*. Since the *edge_ratio* is more favorable, for larger meshes and for a given geometry, the performance is better. The density of the mesh increases faster than the number of cut edges per partition for a given geometry and the computation time predominates the communication time thereby enhancing the performance. The importance of the value of this ratio is well demonstrated with the 32 node machine. In this case the smallest value of the *edge_ratio* corresponds to the aircraft while the immediately greater corresponds to the second largest M6 wing. The performance with the aircraft configuration mesh is about the same as that obtained with the second largest mesh over the M6 wing, since they exhibit similar *edge_ratio*. Yet, this trend seems to disappear when the size of the machine increases: the inherent differences of both meshes are more apparent.

Fig.7 depicts the overall performance for each mesh with respect to the machine configuration. Except for the largest mesh (computed only on the 128 node machine), the performance increases almost linearly with the number of processing nodes. For each mesh, the curves are straight lines with a similar slope, proving again the efficiency of the partitioner. The value of the performance obtained with the smallest mesh on the 64 and 128 node configuration may appear somehow suspicious. In fact, this result is to be expected, since for such a mesh the communication time clearly dominates the computational time.

Finally, while the overall computational rates achieved appear to be rather low, the total time required to obtain a solution is competitive with other unstructured mesh implementations [10, 6]. The simple structure of this explicit algorithm results in a low number of operations for each individual loop. This leads to a high communication/computation ratio on parallel machines, and thus to a low overall computational rate on the CM-5. This is confirmed by the results obtained on the Delta machine [14]: the Delta machine provides communication times smaller than the CM-5, while the CM-5 provides computational times smaller than the Delta through the VU's.

An example of the solution computed over the ONERA M6 wing is depicted Fig.9.

5 CONCLUSION

In this work, it has been shown that the implementation of the 3D Euler solver did not pose any major problems on the CM-5 for the CM Fortran language is very similar for the experienced Fortran-77 programmer. The set of utility subroutines found within the CMSSL library is mostly user-friendly and easy to implement. However, CM Fortran is restrictive in terms of effectiveness. The main drawbacks are:

- Large memory requirements with respect to the size of the problem.
- Large amount of communication, degrading the overall performances to the detriment of rather exceptional pure computational performances.

- Poor communication bandwidth per processing node is not well suited for programs that perform a large amount of inter-processor communication (gather/scatter).

The spectral mesh partitioner implemented in [6] resulted in largely improved solver performance. However, more efficient implementations of the solver and the partitioner demand a thorough understanding of the computer architecture. The solver itself requires a large amount of communication which results in a low overall performance. It is also shown that the communication rates are strongly related to the value of the *edge_ratio*. Improvements could have been achieved either through faster communication rate or through a memory extension of the processors that would allow one to employ larger meshes on the same number of processors.

At last, in [11], the result of a message passing version of their code implemented on the CM-5 reports an overall performance of 102 MFlops for a 786631 edge 2D mesh using 32 processing nodes. While this rate is similar to that achieved in the present work, the former implementation was performed in Fortran-77 and does not make use of the vector units. A message-passing version written in CM Fortran, which would enable the use of the vector units should provide better overall performance.

6 ACKNOWLEDGEMENTS

We warmly thank Zdenek Johan and Earl Renaud for their constant help with the CM Fortran version of this code.

Our thanks extend to the team of Joel Saltz at the University of Maryland at College Park for providing the CM-5 computer access.

Finally, this work completed the postdoctorate year of Eric Morano supported by INRIA, "Région Provence Alpes Côte d'Azur" (FRANCE) and by ICASE (USA).

References

[1] E. Morano, M.H. Lallemand, M.P. Leclercq, H. Steve, B. Stoufflet, and A. Dervieux. Local iterative upwind methods for steady compressible flows. In *GMD-Studien Nr. 189, Multigrid Methods: Special Topics and Applications II*, 1991. Third Conference on Multigrid Methods, Bonn 1990.

[2] E. Morano and A. Dervieux. Looking for $O(N)$ Navier-Stokes solutions on non-structured meshes. In *Sixth Copper Mountain Conference on Multigrid Methods*, pages 449–463. NASA, 1993. NASA CP-3224, Part 2.

[3] Thinking Machine Corporation. *CM Fortran Utility Library Reference Manual, Version 2.0 Beta*, 1993.

[4] Thinking Machine Corporation. *CMSSL for CM Fortran: CM-5 Edition, Volumes I and II, Version 3.1 Beta 2*, 1993.

[5] Thinking Machine Corporation. *CM Fortran Reference Manual, Version 2.0 Beta*, 1992.

[6] Z. Johan, K. Mathur, S. Johnsson, and T. Hughes. An efficient communication strategy for finite element methods on the connection machine CM-5 system. Technical report, Thinking Machine Corporation, 1993. Submitted to Computational Methods in Applied Mechanics and Engineering.

[7] E. Morano and D. Mavriplis. Implementation of a parallel unstructured Euler solver on the CM5. Technical Report 94–0755, AIAA, 1994. 32nd Aerospace Sciences Meeting & Exhibit, January 10-13, Reno, Nevada, USA.

[8] V. Venkatakrishnan, H. Simon, and T. Barth. A MIMD implementation of a parallel Euler solver for unstructured grids. *The Journal of Supercomputing*, 6:117–137, 1992.

[9] C. Farhat, L. Fezoui, and S. Lanteri. Two-dimensional viscous flow computations on the connection machine: unstructured meshes, upwind schemes and massively parallel computations. *Computational Methods in Applied Mechanics and Engineering*, 102:61–88, 1993.

[10] Z. Johan. *Data parallel finite element technique for large-scale computational fluid dynamics.* PhD thesis, Stanford University, 1992.

[11] C. Farhat and S. Lanteri. Simulation of compressible viscous flows on a variety of mpps: Computational algortihms for unstructured dynamic meshes and performance results. Technical Report 2154, INRIA, 1994.

[12] D. Mavriplis. Three dimensional unstructured multigrid for the Euler equations. Technical Report 91-1549CP, AIAA, 1991.

[13] R. Das, D. J. Mavriplis, J. Saltz, S. Gupta, and R. Ponnusamy. The design and implementation of a parallel unstructured Euler solver using software primitives. Technical Report 92-12, ICASE, 1992.

[14] D. Mavriplis. Implementation of a parallel unstructured Euler solver on shared and distributed memory architectures. Technical Report 92-68, ICASE, 1992.

[15] Thinking Machines Corporation. *CMSSL Release Notes, Preliminary Documentation for Version 3.2 Beta*, 1993.

[16] A. Jameson. Numerical solution of the Euler equations for compressible inviscid fluids. In F. Angrand, A. Dervieux, J.A. Désidéri, and R. Glowinski, editors, *Numerical Methods for the Euler Equations of Fluid Dynamics*, pages 199–245. SIAM, Philadelphia, 1985.

Configurations	Nodes	Edges	Boundary Faces
ONERA M6 Wing	2800	17377	2004
ONERA M6 Wing	9428	59863	5864
ONERA M6 Wing	53961	353476	23108
ONERA M6 Wing	357900	2403874	91882
Aircraft	106064	697992	31886

Table 1: Test-case meshes.

Initial Meshes (nodes/edges/b. faces)	Memory (KBytes/VU)	CPU (sec) Partition_Mesh	Total	*Edge_Ratio*	Final Meshes (edges/b. faces)	B. Faces/Edges (%)
2800/17377/2004	324	4.99	17.64	0.77	20480/5120	25.0
9428/59863/5864	604	13.39	51.01	0.43	66560/13312	20.0
53961/353476/23108	2552	78.00	274.63	0.20	360448/48128	13.35
106064/697992/31886	5020	214.80	577.43	0.16	707584/71680	10.13

A. Rule of 8.

Initial Meshes (nodes/edges/b. faces)	Memory (KBytes/VU)	CPU (sec) Partition_Mesh	Total	*Edge_Ratio*	Final Meshes (edges/b. faces)	B. Faces/Edges (%)
2800/17377/2004	260	8.42	21.23	0.79	20480/5120	25.0
9428/59863/5864	408	20.34	57.96	0.43	67584/13312	19.69
53961/353476/23108	1644	127.06	320.83	0.20	360448/48128	13.35
106064/697992/31886	3260	367.73	729.78	0.16	707584/71680	10.13

B. Rule of 8 - Low Storage.

Initial Meshes (nodes/edges/b. faces)	Memory (KBytes/VU)	CPU (sec) Partition_Mesh	Total	*Edge_Ratio*	Final Meshes (edges/b. faces)	B. Faces/Edges (%)
2800/17377/2004	192	4.63	17.48	0.80	18432/3968	21.52
9428/59863/5864	468	12.19	50.31	0.44	61696/11776	19.08
53961/353476/23108	2484	80.44	275.85	0.21	358144/49152	13.72
106064/697992/31886	4948	214.47	572.19	0.16	703104/71168	10.12

C. No Padding.

Initial Meshes (edges/b. faces)	Memory (KBytes/VU)	CPU (sec) Partition_Mesh	Total	*Edge_Ratio*	Final Meshes (edges/b. faces)	B. Faces/Edges (%)
2800/17377/2004	128	6.45	19.36	0.78	18432/4096	22.22
9428/59863/5864	336	18.45	56.74	0.44	61696/11776	19.08
53961/353476/23108	1636	129.91	324.63	0.21	358272/49152	13.71
106064/697992/31886	3252	357.11	719.89	0.16	703744/70784	10.06

D. No Padding - Low Storage.

Table 2: Partitioner Execution Summary - 32 Processing Nodes.

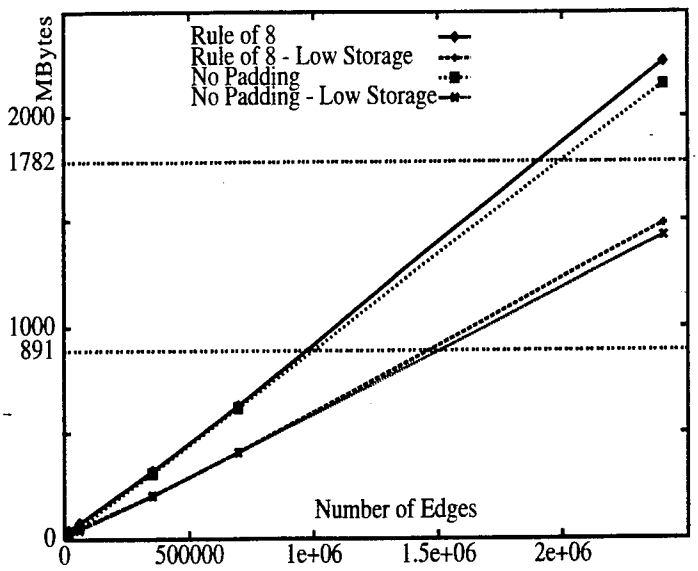

Figure 2: Partitioner's Memory Requirements vs. the Number of Edges - 32 Processing Nodes.

Initial Meshes (nodes/edges/b. faces)	Memory (KBytes/VU)	CPU (sec)		*Edge_Ratio*	Final Meshes (edges/b. faces)	B. Faces/Edges (%)
		Partition_Mesh	Total			
2800/17377/2004	160	3.83	18.93	1.31	18944/5120	27.03
9428/59863/5864	300	8.82	49.29	0.65	62464/14080	22.54
53961/353476/23108	1248	49.01	250.49	0.29	361472/54016	14.94
106064/697992/31886	2476	128.05	501.38	0.22	707840/81664	11.54
357900/2403874/91882 *	5404	759.95	1994.20	0.14	2433280/234240	9.6

(*: low storage)

Table 3: Partitioner Execution Summary - No Padding - 64 Processing Nodes.

Initial Meshes (nodes/edges/b. faces)	Memory (KBytes/VU)	CPU (sec)		*Edge_Ratio*	Final Meshes (edges/b. faces)	B. Faces/Edges (%)
		Partition_Mesh	Total			
2800/17377/2004	84	4.68	22.56	1.93	20992/6144	29.27
9428/59863/5864	184	8.28	53.98	0.91	66560/16384	24.61
53961/353476/23108	692	31.18	248.03	0.41	366592/62464	17.04
106064/697992/31886	1244	72.09	463.74	0.32	714752/123392	11.04
357900/2403874/91882	4140	265.50	1551.57	0.19	2448384/270336	17.26

Table 4: Partitioner Execution Summary - No Padding - 128 Processing Nodes.

Meshes	Memory	CPU 1 Iter (sec)		MFlops
nodes/edges/b. faces	KBytes/VU	Computation	Total	
2800/17377/2004	160	0.022	1.104	13.15
9428/59863/5864	484	0.066	3.705	13.25
53961/353476/23108	2724	0.349	22.649	12.34
106064/697992/31886	5308	0.662	53.858	10.02

Table 5: Euler 3D Solver Execution Summary - Not Partitioned - No Padding - 32 Processing Nodes.

Meshes	Memory	CPU 1 Iter (sec)		MFlops
nodes/edges/b. faces	KBytes/VU	Computation	Total	
2800/20480/5120	216	0.027	0.349	56.90
9428/66560/13312	524	0.078	0.782	77.19
53961/360448/48128	2384	0.379	2.937	104.31
106064/707584/71680	4416	0.714	5.173	112.38

A. Rule of 8.

Meshes	Memory	CPU 1 Iter (sec)		MFlops
nodes/edges/b. faces	KBytes/VU	Computation	Total	
2800/18432/3968	152	0.024	0.312	54.40
9428/61696/11776	452	0.072	0.724	76.72
53961/358144/49152	2320	0.380	2.896	105.51
106064/703104/71168	4412	0.711	5.403	106.92

B. No Padding.

Table 6: Euler 3D Solver Execution Summary - 32 Processing Nodes.

Meshes	Memory	CPU 1 Iter (sec)		MFlops
nodes/edges/b. faces	KBytes/VU	Computation	Total	
2800/18944/5120	76	0.016	0.227	80.94
9428/62464/14080	232	0.039	0.482	120.59
53961/361472/54016	1240	0.202	1.712	182.32
106064/707840/81664	2308	0.366	3.076	191.88
357900/2433280/234240	NOT	FEASIBLE:	OUT OF	MEMORY

Table 7: Euler 3D Solver Execution Summary - No Padding - 64 Processing Nodes.

Meshes	Memory	CPU 1 Iter (sec)		MFlops
nodes/edges/b. faces	KBytes/VU	Computation	Total	
2800/20992/6144	72	0.0111	0.181	114.65
9428/66560/16384	152	0.0235	0.309	203.79
53961/366592/62464	684	0.106	1.021	316.56
106064/714752/123392	1228	0.205	1.773	356.48
357900/2448384/270336	3868	0.622	4.859	417.76

Table 8: Euler 3D Solver Execution Summary - No Padding - 128 Processing Nodes.

Subroutine	Loop Index	Gather (sec)	Computation (sec)	MFlops (C)	Total (sec)	MFlops (T)
STEP	Edges	0.0687	0.0125	688	0.0978	96
	B. Faces	0.0274	0.0061	480	0.0391	78
	Nodes		0.0003	355		
DEFLUX (D)	Edges	0.0798	0.0292	764	0.2234	122
	Nodes		0.0011	228		
DEFLUX (C)	Edges		0.0135	1332	0.1034	209
	B. Faces		0.0087	771	0.0354	216
PSMOO	Edges	0.0580	0.0065	551	0.3589	40
	Nodes		0.0013	585		
MONITR	Nodes		0.0024	218		

Table 9: 1 Iteration, Routine by Routine, Solver's Execution Summary.

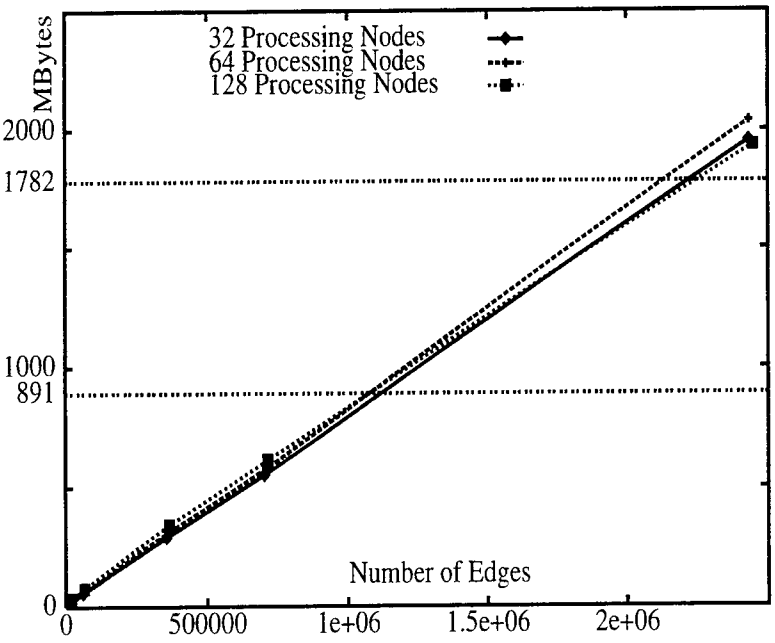

Figure 3: Solver's Memory Requirements vs. the Number of Edges.

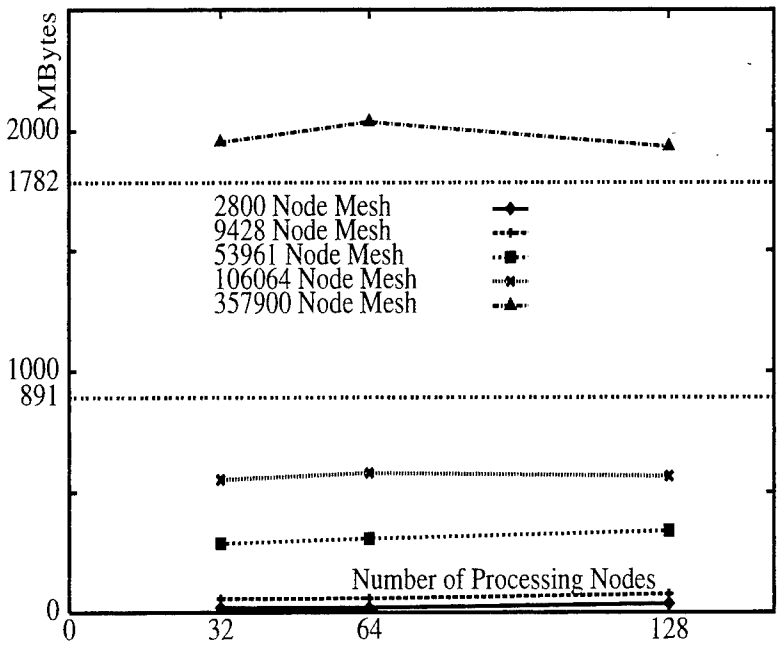

Figure 4: Solver's Memory Requirements vs. the Number of Processing Nodes.

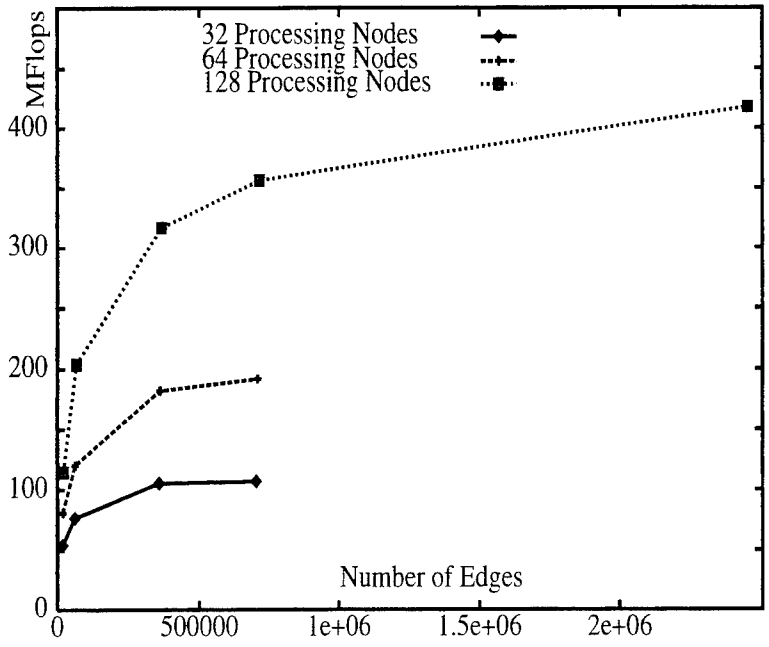

Figure 5: Solver's Overall Performance vs. the Number of Edges.

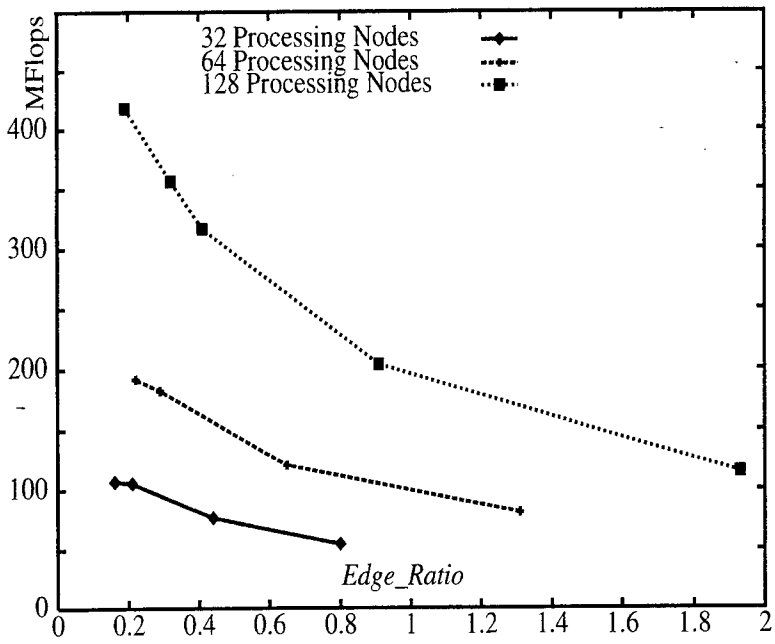

Figure 6: Solver's Overall Performance vs. the Value of the *edge_ratio*.

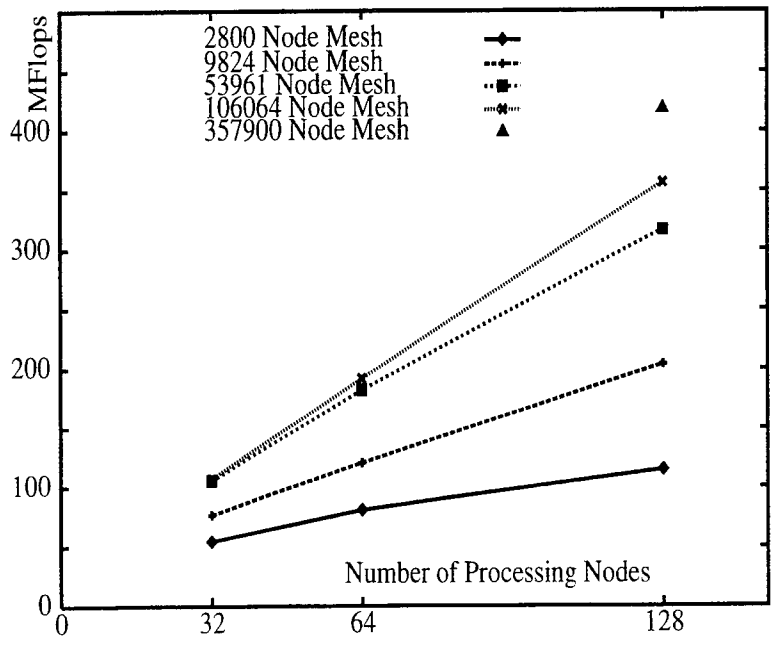

Figure 7: Solver's Overall Performance vs. the Number of Processing Nodes.

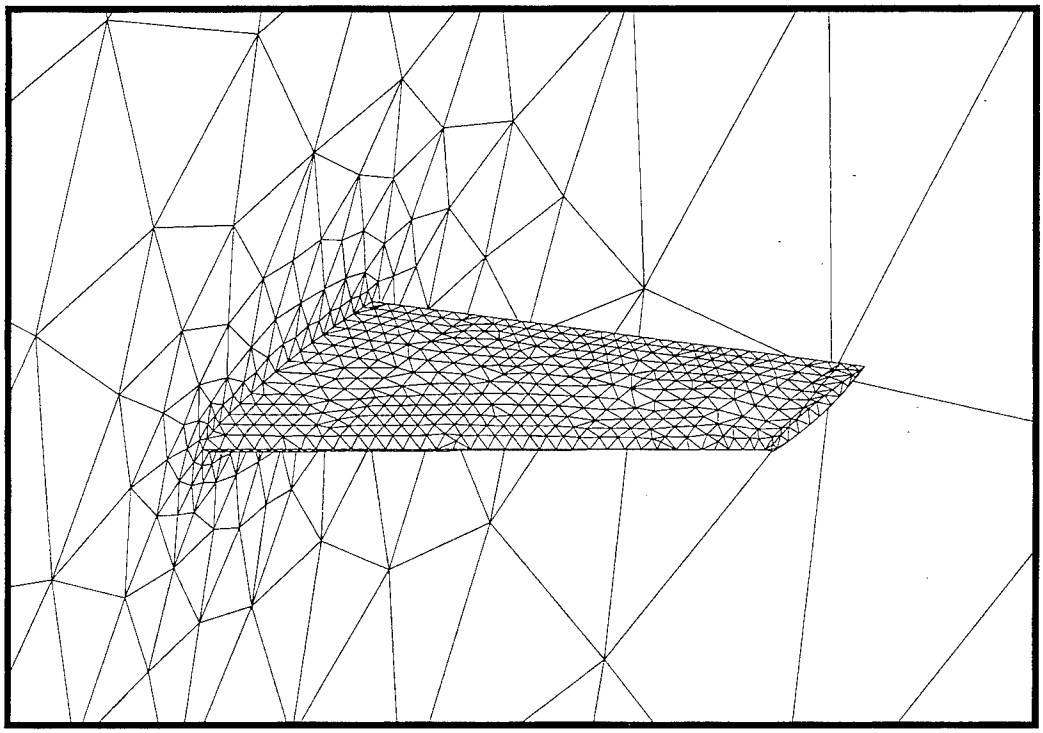

Mesh 1: 2800 Nodes.

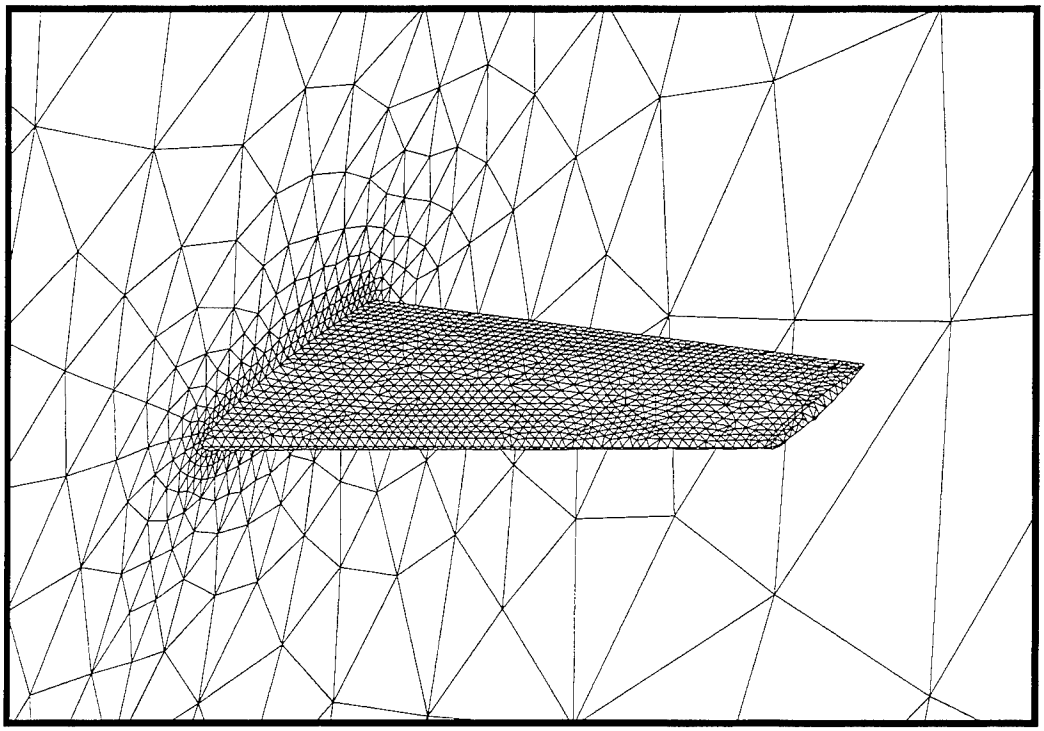

Mesh 2: 9428 Nodes.

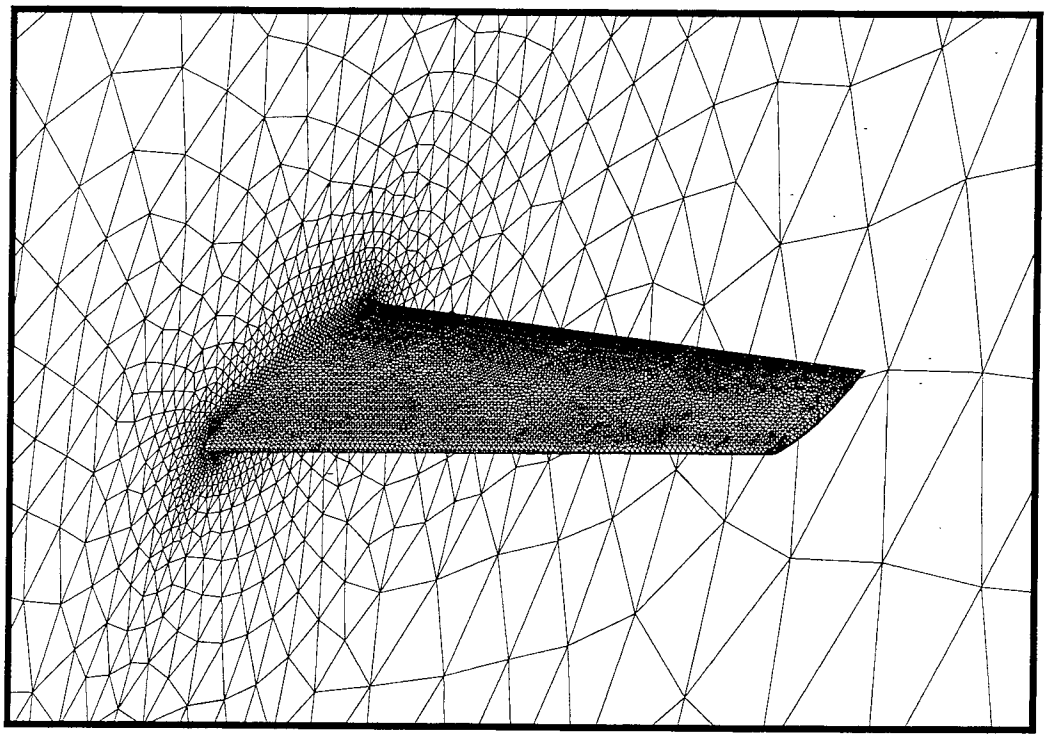

Mesh 3: 53961 Nodes.

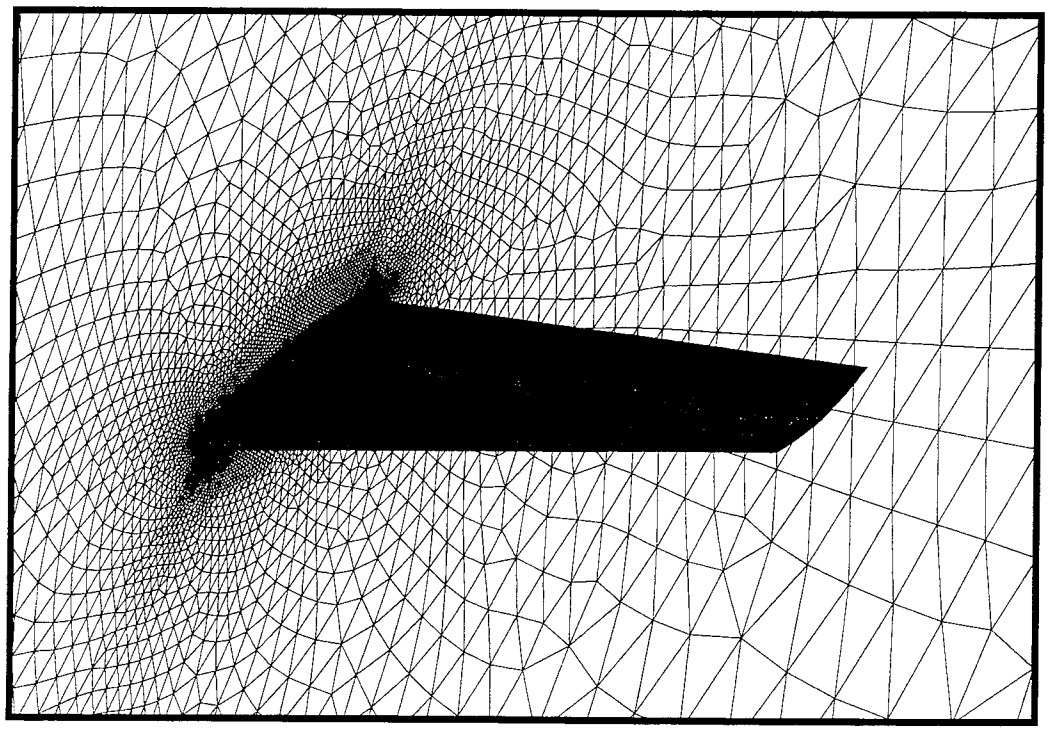

Mesh 4: 357900 Nodes.

Figure 8: Sequence of Meshes Employed for Computing Inviscid Transonic Flow over the ONERA M6 Wing.

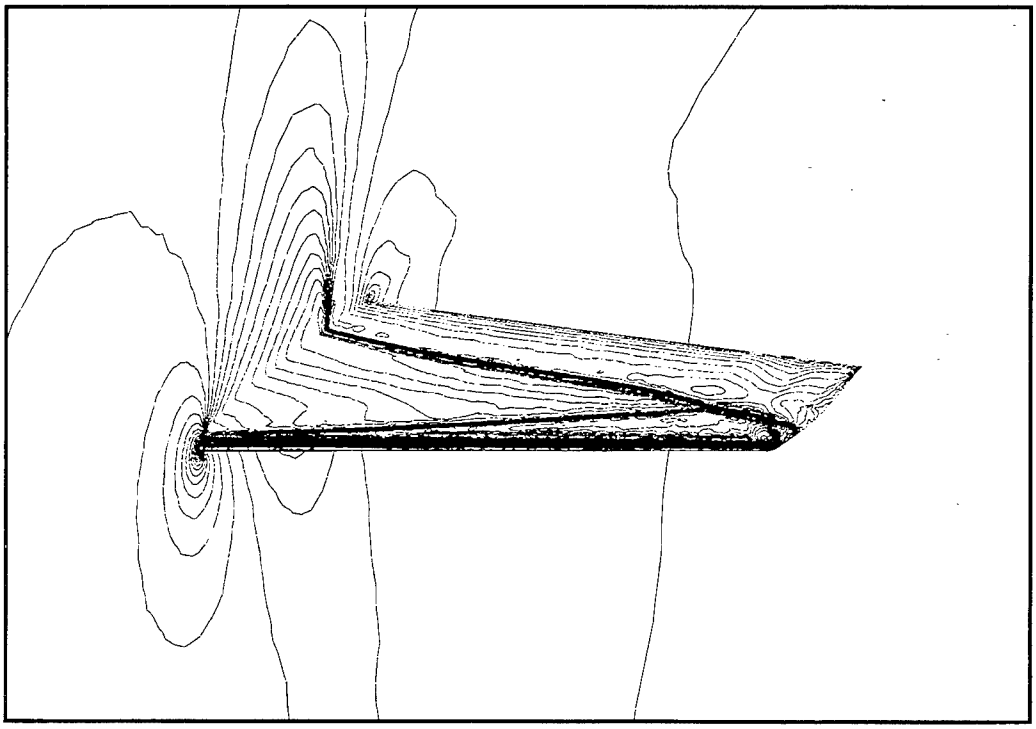

Figure 9: Computed Mach Contours over the 357900 Node ONERA M6 Wing.

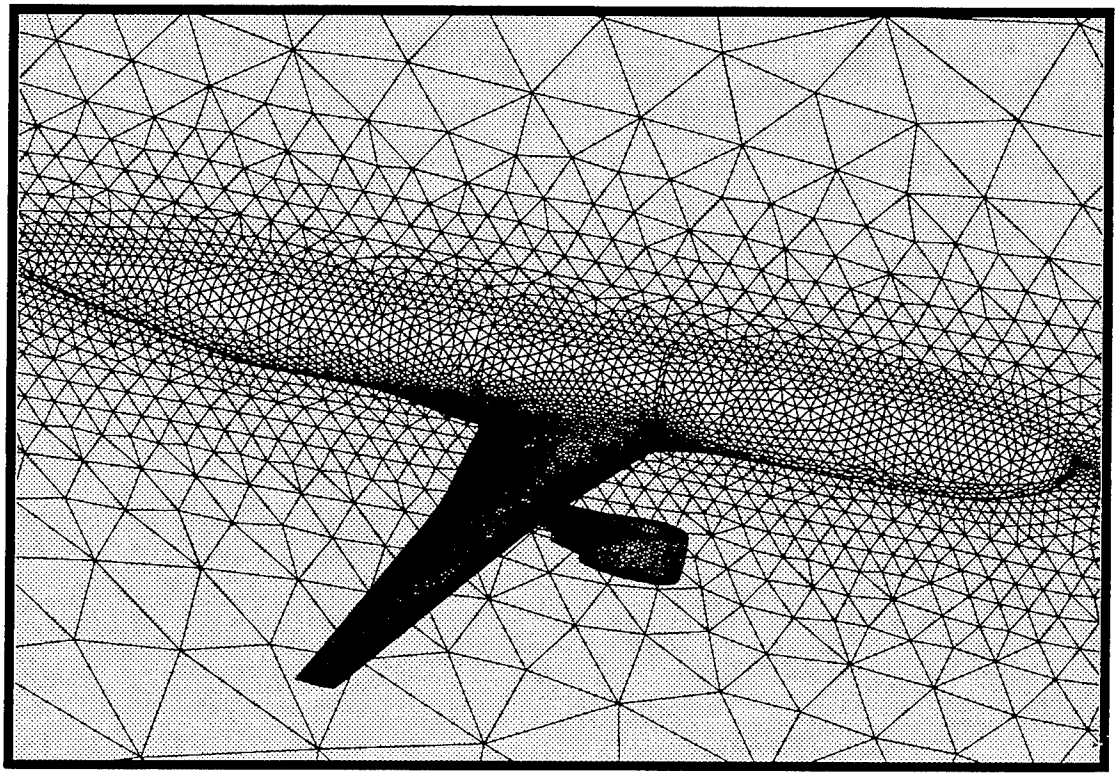

Figure 10: 106064 Node Mesh of a 3D Aircraft Configuration.

REPORT DOCUMENTATION PAGE

Form Approved
OMB No. 0704-0188

1. AGENCY USE ONLY *(Leave blank)*	2. REPORT DATE	3. REPORT TYPE AND DATES COVERED
	March 1995	Contractor Report

4. TITLE AND SUBTITLE
IMPLEMENTATION OF A PARALLEL UNSTRUCTURED EULER SOLVER ON THE CM-5

5. FUNDING NUMBERS
C NAS1-19480
WU 505-90-52-01

6. AUTHOR(S)
E. Morano
D. J. Mavriplis

7. PERFORMING ORGANIZATION NAME(S) AND ADDRESS(ES)
Institute for Computer Applications in Science and Engineering
Mail Stop 132C, NASA Langley Research Center
Hampton, VA 23681-0001

8. PERFORMING ORGANIZATION REPORT NUMBER
ICASE Report No. 95-16

9. SPONSORING/MONITORING AGENCY NAME(S) AND ADDRESS(ES)
National Aeronautics and Space Administration
Langley Research Center
Hampton, VA 23681-0001

10. SPONSORING/MONITORING AGENCY REPORT NUMBER
NASA CR-195056
ICASE Report No. 95-16

11. SUPPLEMENTARY NOTES
Langley Technical Monitor: Dennis M. Bushnell
Final Report
To be submitted to the International Journal of Computational Fluid Dynamics

12a. DISTRIBUTION/AVAILABILITY STATEMENT
Unclassified–Unlimited

Subject Category 64

12b. DISTRIBUTION CODE

13. ABSTRACT *(Maximum 200 words)*
An efficient unstructured 3D Euler solver is parallelized on a Thinking Machine Corporation Connection Machine 5, distributed memory computer with vectorizing capability. In this paper, the SIMD strategy is employed through the use of the CM Fortran language and the CMSSL scientific library. The performance of the CMSSL mesh partitioner is evaluated and the overall efficiency of the parallel flow solver is discussed.

14. SUBJECT TERMS
CM-5; Parallel; SIMD; CMF; CMSSL; Unstructured; 3D Euler

15. NUMBER OF PAGES
22

16. PRICE CODE
A03

17. SECURITY CLASSIFICATION OF REPORT	18. SECURITY CLASSIFICATION OF THIS PAGE	19. SECURITY CLASSIFICATION OF ABSTRACT	20. LIMITATION OF ABSTRACT
Unclassified	Unclassified		